

Charge ordering in Ir dimers in the ground state of $\text{Ba}_5\text{AlIr}_2\text{O}_{11}$

Vamshi M. Katukuri,^{1,*} Xingye Lu,^{2,3,†} D. E. McNally,² Marcus Dantz,² Vladimir N. Strocov,² M. Moretti Sala,⁴ M. H. Upton,⁵ J. Terzic,^{6,7} G. Cao,^{6,7} Oleg V. Yazyev,¹ and Thorsten Schmitt^{2,‡}

¹*Institute of Physics, École Polytechnique Fédérale de Lausanne (EPFL), CH-1015 Lausanne, Switzerland*

²*Swiss Light Source, Photon Science Division, Paul Scherrer Institut, CH-5232 Villigen PSI, Switzerland*

³*Center for Advanced Quantum Studies and Department of Physics, Beijing Normal University, Beijing 100875, China*

⁴*European Synchrotron Radiation Facility, BP 220, F-38043 Grenoble Cedex, France*

⁵*Advanced Photon Source, Argonne National Laboratory, Argonne, Illinois 60439, USA*

⁶*Department of Physics and Astronomy, University of Kentucky, Lexington, Kentucky 40506, USA*

⁷*Department of Physics, University of Colorado at Boulder, Boulder, CO 80309*

(Dated: February 4, 2021)

It has been well established experimentally that the interplay of electronic correlations and spin-orbit interactions in Ir^{4+} and Ir^{5+} oxides results in insulating $J_{\text{eff}}=1/2$ and $J_{\text{eff}}=0$ ground states, respectively. However, in compounds where the structural dimerization of iridium ions is favourable, the direct Ir d - d hybridisation can be significant and takes a key role. Here, we investigate the effects of direct Ir d - d hybridisation in comparison with electronic correlations and spin-orbit coupling in $\text{Ba}_5\text{AlIr}_2\text{O}_{11}$, a compound with Ir dimers. Using a combination of *ab initio* many-body wave function quantum chemistry calculations and resonant inelastic X-ray scattering (RIXS) experiments, we elucidate the electronic structure of $\text{Ba}_5\text{AlIr}_2\text{O}_{11}$. We find excellent agreement between the calculated and the measured spin-orbit excitations. Contrary to the expectations, the analysis of the many-body wave function shows that the two Ir (Ir^{4+} and Ir^{5+}) ions in the Ir_2O_9 dimer unit in this compound preserve their local J_{eff} character close to $1/2$ and 0 , respectively. The local point group symmetry at each of the Ir sites assumes an important role, significantly limiting the direct d - d hybridisation. Our results emphasize that minute details in the local crystal field (CF) environment can lead to dramatic differences in electronic states in iridates and $5d$ oxides in general.

Dimerization or clustering of TM atoms is observed in many TM compounds, e.g. in vanadium oxides [1, 2] and titanates [3] where dimers of spin singlets akin to the Peierls state in one dimension [4] are stabilized when the t_{2g} orbitals of the TM d -manifold are partially filled. In these systems, the TM ions tend to have a strong direct (intra-dimer) d - d overlap that result in molecular-like orbitals with appreciable bonding-antibonding splitting. Consequently, the local electronic structure depends on the intra-dimer hopping integral (t_d), intra-atomic Hund's coupling (J_H) and inter-atomic (U) Coulomb interactions and electron filling of the orbitals localized at TM clusters. Alternatively, dimerization of TM ions can also be favourable from crystallographic considerations, particularly in compounds with heavy TM ions, e.g. $5d$ ions, where the d orbitals are more spread out. A number of dimerized or cluster $4d$ and $5d$ compounds [5–8] with intriguing properties have been synthesized recently. Novel physical phenomena have been observed in these compounds, e.g. the inelastic X-ray scattering analogue of Young's double slit experiment has been realized in $\text{Ba}_3\text{CeIr}_2\text{O}_9$ [9], where the molecular orbital formation within the Ir dimers is crucial. In lacunar spinels GaM_4X_8 ($M=\text{Nb, Mo, Ta}$ and W and $X=\text{S, Se}$ and Te), spin-orbit coupled molecular J_{eff} states [10, 11] and topological superconductivity [12] have been proposed where molecular orbital formation within the tetrahedral cluster of M ions is the key.

The interplay of inter-site electron hopping (t), J_H ,

U and the strong atomic spin-orbit coupling (SOC) in $5d$ and in some $4d$ compounds result in the J_{eff} physics [13–17]. For instance, in compounds with Ir^{4+} (d^5) configuration in an octahedral environment, e.g. in Sr_2IrO_4 [13, 14], the strong SOC leads to completely filled $J_{\text{eff}} = 3/2$ and half-filled $J_{\text{eff}} = 1/2$ levels. Similarly, in Ba_2YIrO_6 and NaIrO_3 , the Ir^{5+} ions realise a completely filled $J_{\text{eff}} = 3/2$ and empty $J_{\text{eff}} = 1/2$ sub-manifolds [18, 19], resulting in a non-magnetic $J_{\text{eff}} = 0$ ground state [20]. In dimerized systems, t_d can be much larger and successively may play a dominant role compared to other local interactions, which could result in the breakdown or a significant modification of the J_{eff} physics. Thus, it is crucial to identify the role of these multiple physical interactions in Ir dimer systems to gain a better understanding of the electronic and magnetic properties of these materials.

In this letter, we illustrate how subtle crystal structure details are extremely important to precisely understand the electronic structure of $5d$ compounds where structural dimerization or clustering is prevalent. Using state-of-the-art *ab initio* many-body electronic structure methods in combination with high-resolution resonant inelastic X-ray scattering (RIXS) experiments, we present a detailed analysis of the electronic structure of Ir_2O_9 dimers in $\text{Ba}_5\text{AlIr}_2\text{O}_{11}$ and unravel the nature of electronic ground and excited states of $\text{Ba}_5\text{AlIr}_2\text{O}_{11}$. While we find an excellent agreement between the RIXS spectra and the calculated excitations, analysis of the many-body

wave functions reveal a nearly complete charge separation – Ir^{4+} and Ir^{5+} – within the dimers in the ground state, in contrary to an earlier report of formation of molecular orbitals in $\text{Ba}_5\text{AlIr}_2\text{O}_{11}$ [21]. The strong SOC of the Ir^{4+} and Ir^{5+} ions results in $J_{\text{eff}} = 1/2$ and $J_{\text{eff}} = 0$ local configurations, respectively, and thus we conclude that a localized J_{eff} picture is more appropriate in $\text{Ba}_5\text{AlIr}_2\text{O}_{11}$.

$\text{Ba}_5\text{AlIr}_2\text{O}_{11}$ contains dimers composed of crystallographically inequivalent Ir cations engaged in face sharing O_6 octahedra [22, 23], see Fig. 3a and 3b, and Supplementary material (SM) Fig. S1 [24]. At 210 K, a lattice distortion is believed to lower the symmetry of the crystal and enhance the charge disproportionation leading to charge ordering that correspond to Ir^{4+} and Ir^{5+} valence configurations [23]. However, analysis of RIXS spectrum of $\text{Ba}_5\text{AlIr}_2\text{O}_{11}$ using density functional theory and model Hamiltonian calculations [21] has proposed the formation of hybridized dimer orbitals, debunking the charge disproportionation phenomenon. Nevertheless, given the complex low-symmetry crystal environment and the interplay of spin and orbital degrees of freedom in $\text{Ba}_5\text{AlIr}_2\text{O}_{11}$, it is unclear if the dimer orbitals are actually realised in the ground state.

Results: The RIXS spectra shown in Fig. 1 was measured on single crystals grown by flux method [23] at the ID20 beam line of the European Synchrotron Radiation Facility (ESRF) with ~ 25 meV resolution [25] and the 27-ID-B beamline with ~ 30 meV resolution at the Advanced Photon Source (APS), with π polarization at a scattering angle close to $2\theta = 90^\circ$. The incident-energy dependence of RIXS spectra across the Ir- L_3 edge ($E_i = 11.215\text{keV}$) at the zone center $Q=(23.5, 0, 2.5)$ is shown in Fig. 1(a). While the same E_i as determined from previous measurements on iridates such as Sr_2IrO_4 and Ba_2YIrO_6 [20, 26] was chosen, we find that the maximum of the resonance is not at E_i in $\text{Ba}_5\text{AlIr}_2\text{O}_{11}$ as the precise CF environment around Ir ions and the mixing of the valence states influences the resonance energy. However, we see that the energies of the modes remain unchanged in a broad range around E_i .

The features marked by A-K in Fig. 1(b) are incident-energy independent Raman modes as shown in Fig. 1(a). These modes correspond to intrinsic electronic transitions between various occupied and unoccupied states, and therefore provide direct information about low energy electronic structure. To resolve all the Raman modes and determine the low energy electronic structure, we show in Figs. 1(b) and 1(c) high statistic energy spectra collected at E_i (white dashed line in Fig. 1(a)). In Fig. 1(b), several sharp Raman modes below 1 eV and a broad peak at 1.2 eV, named A to K are determined by fitting the spectra using multiple Gaussians. The sum of the fitting curves is shown as a green solid curve. In Fig. 1(c), higher energy excitations up to 8 eV are shown. This spectrum is decomposed into several peaks and in-

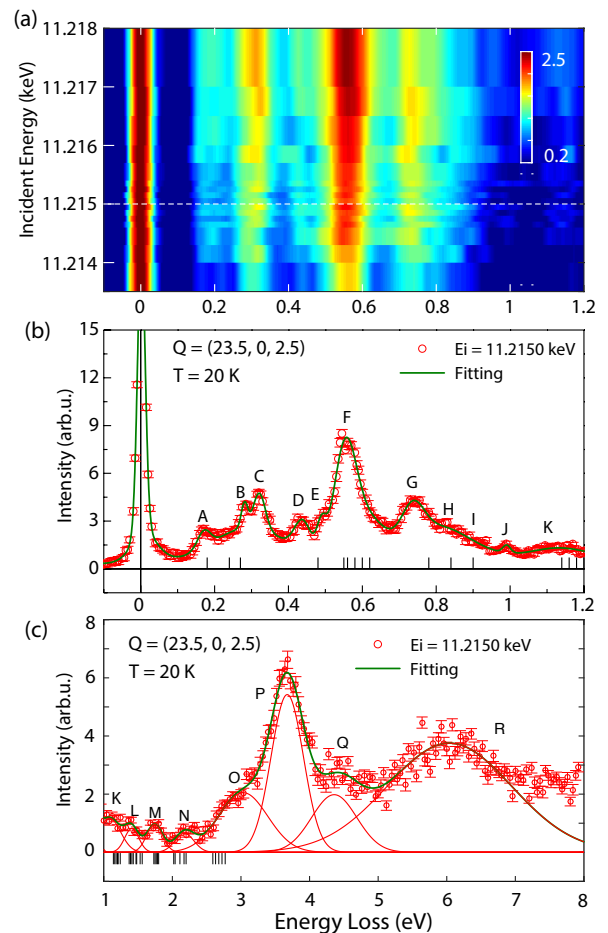


FIG. 1. (a) Incident-energy dependence of elementary excitations below 1.2 eV for $\text{Ba}_5\text{AlIr}_2\text{O}_{11}$ measured around Ir L_3 edge with $Q = (23.5, 0, 2.5)$ at 20 K. (b) RIXS spectra (below 1.2 eV) measured at $E_i = 11.215$ keV (marked as white dashed line in (a)). (c) High energy excitations (1-8 eV) measured with the same setup as that for (b). Green line is a Multi-Gaussian fitting of the raw data in red open circles (with error bars).

terestingly, these modes show very little momentum dependence (see SM Fig. S6 [24]), indicating that all of them correspond to local spin-orbital ($d-d$) excitations and reflecting the low energy electronic structure.

We now turn to the RIXS results measured using O- K edge (Fig. 2 and Fig. S2 in SM [24]) carried out at the ADDRESS beamline of the Swiss Light Source at the Paul Scherrer Institut, with ~ 70 meV energy resolution for both σ and π polarizations at a scattering angle of $2\theta = 130$ deg. [27, 28], see SM, Fig. S1. With the presence of strong hybridization between O $2p$ orbitals and Ir $5d$ orbitals, O- K RIXS is sensitive to various elementary excitations of iridates [29]. Figs. 2(a) and 2(b) are RIXS maps collected at O- K edge with π and σ polarizations at 25° grazing incidence. Besides the sharp spin-orbital excitations ($E \approx 0.26, 0.57$ eV) below 1 eV consistent

with those measured with Ir- L_3 edge, two high energy excitations at $E \approx 2.26$ and 2.71 eV have also been observed. Note the RIXS maps in Fig. 2 contains substantial fluorescence which is absent in the results collected at Ir L_3 edge (Fig. 1), indicating complex energy levels/bands of oxygen ions. In addition, significant polarization dependence of the excitations have also been observed, which we attribute to the overlap between light polarization (electric field \mathbf{E}) and the different O $2p$ orbitals hybridized with different Ir $5d$ orbitals (for details, see [24]).

To decipher the nature of the rich excitation spectrum observed in RIXS spectra and to examine the formation of dimer orbitals in $\text{Ba}_5\text{AlIr}_2\text{O}_{11}$, we performed many-body *ab initio* cluster-in-embedding quantum chemistry (QC) calculations, starting from the crystal structure reported in Ref. [22, 23]. These are based on the construction of the exact wave function for the atoms in the cluster using configuration interaction wave function theory –

TABLE I. Relative energies (eV) of the excitation levels calculated at CASSCF+NEVPT2 level of theory. The first column contains non-relativistic multiplet structure, the multiplet symbols on the left correspond to the octahedral (O_h) symmetry. The degeneracy of the states is split in $\text{Ba}_5\text{AlIr}_2\text{O}_{11}$ due to the lowered symmetry in the two octahedra due to the anisotropic crystal fields, see text. Spin-orbit coupled multiplet structure is shown in the second column. Note that each state is doubly degenerate (Kramers doublet). The corresponding peaks in the RIXS data in Fig. 1a are shown in column 3.

CASSCF+NEVPT2	+ SOC (x 2)	Ir L-edge RIXS
$^4A_1 - 0.00$	0.00	0.00
$^2T_1 - 0.03, 0.08, 0.10$	0.18	0.18 (A)
$^2A_1 - 0.14$	0.24, 0.27	0.28 (B) 0.33 (C)
$^4T_1 - 0.16, 0.17, 0.17$		0.44 (D)
$^2E_1 - 0.18, 0.23$	0.48, 0.62	0.50 (E)
$^4E_1 - 0.25, 0.28$	0.55, 0.56, 0.58	0.56 (F)
$^2T_2 - 0.77, 0.80, 0.94$	0.60, 0.78	0.75 (G)
$^4T_2 - 0.84, 0.86, 0.95$	0.84, 0.90	0.82 (H)
$^2T_3 - 0.86, 0.86, 0.90$	1.14 – 1.20 (4)	0.98 (I), 1.00 (J)
$^2A_2 - 0.91$	1.21, 1.24	1.20 (K)
$^2E_2 - 1.00, 1.01$	1.37 – 1.43 (4)	1.4 (L)
$^2A_3 - 1.03$	1.47	
$^2T_4 - 1.10, 1.10, 1.12$	1.48, 1.53, 1.56	
$^2E_3 - 1.60, 1.63$	1.73 – 1.80 (5)	1.77 (M)
$^2T_5 - 1.68, 1.78, 1.81$	2.02, 2.04	
	2.11, 2.17, 2.20	2.17 (N)
	2.59	
	2.63 – 2.77 (4)	2.70 (O)

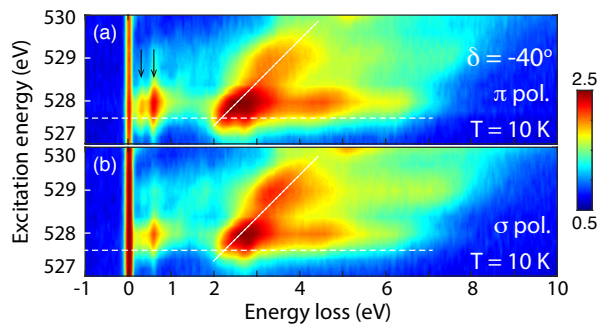


FIG. 2. RIXS results of $\text{Ba}_5\text{AlIr}_2\text{O}_{11}$ as measured at O- K edge. (a, b) Energy dependence of RIXS spectra for $\text{Ba}_5\text{AlIr}_2\text{O}_{11}$ taken around O- K edge with $\delta = -40^\circ$ ($Q = (0.93, 0, 0.65)$).

complete active space self-consistent field (CASSCF) and multireference perturbation methods [30]. The calculations were performed on a cluster containing one Ir_2O_9 dimer unit, two neighboring AlO_4 tetrahedra and the surrounding 15 Ba^{2+} ions. All the calculations were performed using ORCA quantum chemistry program [31], see SM [24] for all the computational details.

Relative energies of the multiplet structure of the Ir_2O_9 dimer unit obtained from CASSCF + NEVPT2 (N-electron valence perturbation theory) [32] calculations are shown in Table I. An active space of nine electrons in six orbitals (three t_{2g} orbitals on each iridium) was considered in the CASSCF calculation which sufficiently captures the important static correlations (i.e. near degeneracies) in $\text{Ba}_5\text{AlIr}_2\text{O}_{11}$. In the NEVPT2 calculation, the correlations involving all the neighboring occupied oxygen $2p$ and iridium $5s, 5p$ orbitals as well as all the unoccupied orbitals are accounted for, accurately describing the O-2p to Ir-d charge transfer effects and other dynamic correlation effects. It is important to note that the intra- (Hund's coupling J_H) and inter-site (U) Coulomb interactions and the hybridization between different orbitals are included in the calculation, accurate within the basis-set limit.

The lowest nine quartet ($s = \frac{3}{2}$) and 24 doublet ($s = \frac{1}{2}$) scalar relativistic states (first column in Table I) are first computed and then are allowed to admix via the SOC, resulting in 84 states, see the second column of Table I. It can be seen that the excitation energies obtained from CASSCF+NEVPT2+SOC calculations are in excellent agreement with the peaks observed in RIXS experiments, except for peak D. This peak is related to the electron-hole exciton which is also observed in other iridate materials such as Sr_2IrO_4 [29, 33] and Na_2IrO_3 [34]. Such excitations are not considered in the current QC calculations[35]. Further, our calculations reveal excitations from the t_{2g} to e_g manifold starting at 3.4 eV which correspond to RIXS peaks P and Q.

To elucidate the origin of these excitations, we first

analyze the scalar-relativistic multiplet structure. When the two iridium ions in the dimer unit are in cubic environment (O_h symmetry), the low energy multiplet structure is a result of the interaction of the ground state ${}^2T_{1g}$ multiplet of the Ir^{4+} ion [36] and the ${}^3T_{1g}$ ground state term of the Ir^{5+} ion. In addition, the lowest ${}^1T_{1g}$ and ${}^1E_{1g}$ [20] singlet states contribute significantly to the low energy spin-orbit excitations [20]. The resulting spectrum contains ${}^4T_{1g}$, ${}^4T_{2g}$, ${}^4A_{1g}$, ${}^4E_{1g}$, quartets and 11 doublet terms $-{}^2T_{1g,2g,3g,4g,5g}$, ${}^2A_{1g,2g,3g}$, ${}^2E_{1g,2g,3g}$ [37]. However, in $\text{Ba}_5\text{Allr}_2\text{O}_{11}$ the Ir ions are enclosed in distorted octahedra resulting in low symmetry CFs and splitting of the t_{2g} levels at each Ir ion [38]. Further, the small Ir-Ir intra-dimer distance of 2.73 Å in $\text{Ba}_5\text{Allr}_2\text{O}_{11}$ (2.698 Å in elemental iridium) may result in direct overlap of the Ir d orbitals and the formation of bonding and antibonding states [39]. Consequently, the multiplet degeneracies in the spectrum are split.

To understand the formation of bonding and antibonding dimer orbitals in $\text{Ba}_5\text{Allr}_2\text{O}_{11}$, we plot the evolution of orbital energies as a function of Ir_1 - Ir_2 intra-dimer distance (d) in Fig. 3(c). The six levels for each d correspond to the CASSCF canonical orbital [40] energies of the six t_{2g} -like orbitals in the Ir_2O_9 dimer unit. The colour variations of the energy levels represent the orbital compositions [41] from Ir_1 , Ir_2 and O ions. Interestingly, for $d \geq 2.73$ Å, we find 20% and 13% hybridization for Ir_1 $5d - \text{O } 2p$ and Ir_2 $5d - \text{O } 2p$, respectively, while there is negligible direct Ir_1 - Ir_2 d -orbital hybridization. The a_{1g} orbital of Ir_1 contains 4.5% contribution from a_{1g} orbital of Ir_2 and vice versa. For $d = 2.65$ Å, a significant direct Ir_1 - Ir_2 d -orbital hybridization is observed. We find this hybridization increasing up to 25% for $d = 2.45$ Å, resulting in large bonding – antibonding energy separation, as seen in the corresponding orbital plots in Fig. 3(d). Note that for $d = 2.73$ Å orbitals with predominantly Ir_1 character are at higher energies than those of Ir_2 character, reflecting different on-site orbital energies. This is a direct consequence of the difference in the valence configurations of Ir_1 and Ir_2 ions and the $\text{Ir}_{1,2} 5d - \text{O } 2p$ hybridization.

The effect of the low crystal field symmetry at two different Ir ions can be estimated by computing the t_{2g} splittings, δ , at each of the Ir ions from restricted active space (RAS) [42] calculations where the d orbital occupation at the other Ir ion is constrained. We find considerably large t_{2g} splittings of $\delta_1 = 0.58$ and $\delta_2 = 0.60$ eV for Ir_1 and Ir_2 , respectively. Such large values compete with the SOC strength of ~ 0.5 eV of the Ir ions to considerably reduce the effect of SOC, thus resulting in the modification of the local spin-orbit multiplet structure.

The scalar-relativistic ground state realized in $\text{Ba}_5\text{Allr}_2\text{O}_{11}$ is the double exchange ${}^4A_{1g}$ multiplet [43], an orbitally non-degenerate high-spin quartet, with wave function ${}^4\psi_0 = \alpha|d_1^4, d_2^5\rangle + \beta|d_1^3, d_2^6\rangle + \gamma|d_1^5, d_2^4\rangle$ with $\alpha^2 = 0.89$, $\beta^2 = 0.09$ and $\gamma^2 = 0.02$, where d_i^n cor-

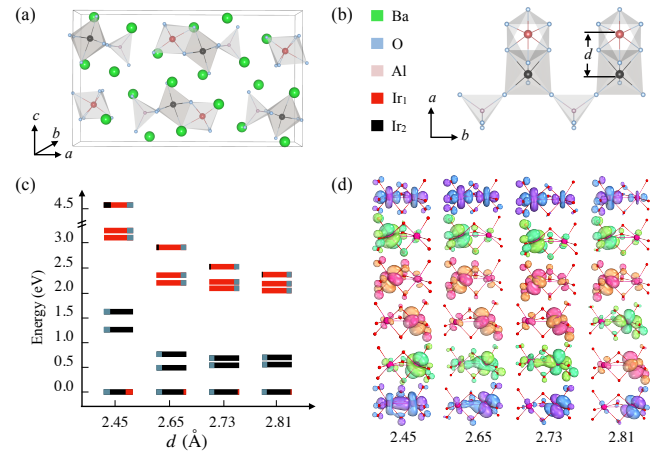


FIG. 3. Crystal structure of $\text{Ba}_5\text{Allr}_2\text{O}_{11}$: (a) unit cell, (b) Ir_2O_9 dimer units connected along b . d is the intra-dimer Ir_1 - Ir_2 distance. (c) Orbital (relative) energy-level diagram of the six t_{2g} orbitals, shown in (d), for different d , the lowest energy orbital is set to zero. The length of red, black and blue colours of each level are proportional to the percentage contributions from Ir_1 , Ir_2 and O ions, respectively.

responds to n electrons in Ir_i d orbitals. The lowest 2T_1 doublet state is 40 meV higher with wave function weights $\alpha^2 = 0.85$, $\beta^2 = 0.11$ and $\gamma^2 = 0.02$. We further find that the weight of $|d_1^4, d_2^5\rangle$ configuration in all the excited multiplet wave functions is greater than 95%. It is interesting to note that excluding all the configurations involving hopping of electrons from Ir_1 to Ir_2 and vice versa in the wave function preserve the spin-orbit spectrum except for an overall shift ≤ 50 meV. The double exchange ground state as well as the dominant contribution of $|d_1^4, d_2^5\rangle$ configuration imply charge separation within the dimer units. Further, the natural orbital occupations obtained from the CASSCF calculations are close to 4 and 5 for Ir_1 and Ir_2 ions, respectively. Thus, we conclude that the two Ir ions in $\text{Ba}_5\text{Allr}_2\text{O}_{11}$ host different ionic states – Ir_1^{5+} and Ir_2^{4+} – which results in charge ordering within the dimers and the low energy excitations are strictly local to individual Ir ions and not among dimer orbitals.

The SOC results in the admixture of all the 15 non-relativistic multiplet terms shown in Table I. Addition of angular momenta of two $l_{\text{eff}}=1$ ($l_{\text{eff},1} = l_{\text{eff},2} = 1$) sites with spins $s_1 = 1/2$ and $s_2 = 1$ gives rise to 84 effective total angular momentum (J_{eff}) states. In $\text{Ba}_5\text{Allr}_2\text{O}_{11}$, due to the non-cubic CFs, all degeneracies are removed except for the Kramers doublet degeneracy. From the analysis of the wave functions, we assign the peaks A-C to excitations from the Ir_1 $J_{\text{eff}} = 0$ to $J_{\text{eff}} = 1$ states. The peak F and satellite feature H consists of excitations from Ir_1 $J_{\text{eff}} = 0$ to $J_{\text{eff}} = 2$ and Ir_2 $J_{\text{eff}} = 1/2$ to $J_{\text{eff}} = 3/2$ states that are split due to non-cubic CFs. The peak G originates from excitations involving Ir_1 $J_{\text{eff}} = 0$ and $J_{\text{eff}} = 2$ states as well. The peaks I-K are the result of

simultaneous on-site excitations at Ir₁ and Ir₂ ions, see Fig. S5 in SM [24].

At the first sight, an insignificant Ir-Ir intra-dimer d -orbital hybridization in Ba₅Allr₂O₁₁ might be surprising, even though the distance between Ir sites is close to that of Ir metal. However, due to the crystallographic in-equivalence of the two Ir ions in the dimer unit and the different O₆ arrangement, the symmetry of split t_{2g} orbitals at each of the Ir ions is very different and subsequently a little direct overlap is realized. In fact, for dimer systems with structurally equivalent ions such as Ba₃InIr₂O₉ [7], we find a considerable hybridization resulting in delocalized dimer orbitals [44]. It would be interesting to characterize the local electronic structure in other face-sharing Ir-dimer compounds such as Ba₃ZnIr₂O₉ and Ba₃ZrIr₂O₉ [45] where the Ir dimer unit occupancy is eight and ten respectively.

In conclusion, we have measured both Ir L_3 and O K -edge RIXS spectra and observed multiple spin-orbital excitations. Our *ab initio* quantum chemistry calculations reproduce very well the excitation spectrum up to 3.5 eV observed in the RIXS measurements. We find charge ordering within the Ir-dimers with Ir₁⁵⁺(d^4) and Ir₂⁴⁺(d^5) configurations. We have established a direct connection between the excitations in Ir₂O₉ dimer unit and those at individual Ir ions. The appearance of multiple peaks is a direct consequence of strong non-cubic CFs originating from the distorted octahedral environment around the Ir ions. In spite of small intra-dimer Ir-Ir distance, the direct d - d hybridization is relatively weak and the bonding-antibonding splitting is negligible compared to the non-cubic CF splittings. Alternatively, we find increased intra-dimer configuration mixing due to strong electron-electron interactions, particularly the $|d_1^3, d_2^6\rangle$ configuration stabilizing the ground state. This strongly supports nearly complete charge ordering within the Ir dimers in Ba₅Allr₂O₁₁ and refutes the suggested formation of dimer orbitals [21]. Our results highlight the importance of minute details of the crystal structure to understand the electronic and magnetic properties of clustered Iridates and TM magnets in general and calls for re-investigating several already studied materials with accurate *ab initio* many-body calculations. Finally, we emphasize that the combination of RIXS and quantum chemistry calculations is an excellent tool to unambiguously decipher complicated electronic structures.

V. M. K. and O. V. Y. would like to acknowledge funding from Swiss NSF NCCR MARVEL and the Sinergia grant NanoSkyrmionics CR- SII5 171003. The work at PSI is supported by the Swiss NSF through the NCCR MARVEL and the Sinergia network Mott Physics Beyond the Heisenberg Model (MPBH). X. L. acknowledges financial support from the European Community's Seventh Framework Programme (FP7/20072013) under Grant agreement No. 290605 (Cofund; PSI-Fellow). The work at BNU is supported by the National Natural Sci-

ence Foundation of China under Grant No. 11734002 and 11922402. M. D. was partially funded by the Swiss National Science Foundation within the D-A-CH programme (SNSF Research Grant 200021L 141325). This research used resources of the Advanced Photon Source, a U.S. Department of Energy (DOE) Office of Science User Facility operated for the DOE Office of Science by Argonne National Laboratory under Contract No. DE-AC02-06CH11357.

* Current address: Max Planck Institute for Solid State Physics, Heisneberstrasse 1, 70569, Stuttgart Germany; V.Katukuri@fkf.mpg.de

† luxy@bnu.edu.cn

‡ thorsten.schmitt@psi.ch

- [1] Masatoshi Imada, Atsushi Fujimori, and Yoshinori Tokura, "Metal-insulator transitions," *Rev. Mod. Phys.* **70**, 1039–1263 (1998).
- [2] H. F. Pen, J. van den Brink, D. I. Khomskii, and G. A. Sawatzky, "Orbital Ordering in a Two-Dimensional Triangular Lattice," *Phys. Rev. Lett.* **78**, 1323–1326 (1997).
- [3] D. I. Khomskii and T. Mizokawa, "Orbitally Induced Peierls State in Spinels," *Phys. Rev. Lett.* **94**, 156402 (2005).
- [4] R. Peierls, *More Surprises in Theoretical Physics* (Princeton University Press, 1991).
- [5] Ichiro Terasaki, Shun Ito, Taichi Igarashi, Shinichiro Asai, Hiroki Taniguchi, Ryuji Okazaki, Yukio Yasui, Kensuke Kobayashi, Reiji Kumai, Hironori Nakao, and Youichi Murakami, "Novel Charge Ordering in the Trimer Iridium Oxide BaIrO₃," *Crystals* **6** (3), 27 (2016).
- [6] Abhishek Nag, S. Middey, Sayantika Bhowal, S. K. Panda, Roland Mathieu, J. C. Orain, F. Bert, P. Mendels, P. G. Freeman, M. Mansson, H. M. Ronnow, M. Telling, P. K. Biswas, D. Sheptyakov, S. D. Kaushik, Vasudeva Siruguri, Carlo Meneghini, D. D. Sarma, Indra Dasgupta, and Sugata Ray, "Origin of the Spin-Orbital Liquid State in a Nearly $J = 0$ Iridate Ba₃ZnIr₂O₉," *Phys. Rev. Lett.* **116**, 097205 (2016).
- [7] Tusharkanti Dey, M. Majumder, J. C. Orain, A. Senyshyn, M. Prinz-Zwick, S. Bachus, Y. Tokiwa, F. Bert, P. Khuntia, N. Büttgen, A. A. Tsirlin, and P. Gegenwart, "Persistent low-temperature spin dynamics in the mixed-valence iridate Ba₃InIr₂O₉," *Phys. Rev. B* **96**, 174411 (2017).
- [8] Abhishek Nag, Sayantika Bhowal, F. Bert, A. D. Hillier, M. Itoh, Ilaria Carlomagno, C. Meneghini, T. Sarkar, R. Mathieu, I. Dasgupta, and Sugata Ray, "Ba₃MIr₂O₉ hexagonal perovskites in the light of spin-orbit coupling and local structural distortions," *Phys. Rev. B* **97**, 064408 (2018).
- [9] A. Revelli, M. Moretti Sala, G. Monaco, P. Becker, L. Bohatý, M. Hermanns, T. C. Koethe, T. Fröhlich, P. Warzawski, T. Lorenz, S. V. Streltsov, P. H. M. van Loosdrecht, D. I. Khomskii, J. van den Brink, and M. Grüninger, "Resonant inelastic x-ray incarnation of Young's double-slit experiment," *Sci. Adv.* **5**, eaav4020 (2019).
- [10] Heung-Sik Kim, Jino Im, Myung Joon Han, and Hosub

- Jin, “Spin-orbital entangled molecular j_{eff} states in lacunar spinel compounds,” *Nat Commun* **5**, 3988 (2014).
- [11] Min Yong Jeong, Seo Hyoung Chang, Beom Hyun Kim, Jae-Hoon Sim, Ayman Said, Diego Casa, Thomas Gog, Etienne Janod, Laurent Cario, Seiji Yunoki, Myung Joon Han, and Jung-ho Kim, “Direct experimental observation of the molecular $J_{\text{eff}} = 3/2$ ground state in the lacunar spinel GaTa_4Se_8 ,” *Nat Commun* **8**, 782 (2017).
- [12] Moon Jip Park, GiBaik Sim, Min Yong Jeong, Archana Mishra, Myung Joon Han, and SungBin Lee, “Pressure-induced topological superconductivity in the spin-orbit Mott insulator GaTa_4Se_8 ,” *npj Quantum Mater.* **5**, 41 (2020).
- [13] B. J. Kim, Hosub Jin, S. J. Moon, J. Y. Kim, B. G. Park, C. S. Leem, Jaejun Yu, T. W. Noh, C. Kim, S. J. Oh, J. H. Park, V. Durairaj, G. Cao, and E. Rotenberg, “Novel $J_{\text{eff}} = 1/2$ Mott State Induced by Relativistic Spin-Orbit Coupling in Sr_2IrO_4 ,” *Phys. Rev. Lett.* **101**, 076402–076402 (2008).
- [14] B. J. Kim, H. Ohsumi, T. Komesu, S. Sakai, T. Morita, H. Takagi, and T. Arima, “Phase-Sensitive Observation of a Spin-Orbital Mott State in Sr_2IrO_4 ,” *Science* **323**, 1329–1332 (2009).
- [15] Vamshi M. Katukuri, Hermann Stoll, Jeroen van den Brink, and Liviu Hozoi, “*Ab initio* determination of excitation energies and magnetic couplings in correlated quasi-two-dimensional iridates,” *Phys. Rev. B* **85**, 220402 (2012).
- [16] M. Moretti Sala, S. Boseggia, D.F. McMorro, and G. Monaco, “Resonant X-Ray Scattering and the $J_{\text{eff}} = 1/2$ Electronic Ground State in Iridate Perovskites,” *Phys. Rev. Lett.* **112**, 026403 (2014).
- [17] William Witczak-Krempa, Gang Chen, Yong Baek Kim, and Leon Balents, “Correlated Quantum Phenomena in the Strong Spin-Orbit Regime,” *Annu. Rev. Condens. Matter Phys.* **5**, 57–82 (2014).
- [18] A. Abragam and B. Bleaney, *Electron Paramagnetic Resonance of Transition Ions* (Clarendon Press, Oxford, 1970).
- [19] Giniyat Khaliullin, “Excitonic magnetism in van vleck type d^4 mott insulators,” *Phys. Rev. Lett.* **111**, 197201 (2013).
- [20] M. Kusch, V. M. Katukuri, N. A. Bogdanov, B. Büchner, T. Dey, D. V. Efremov, J. E. Hamann-Borrero, B. H. Kim, M. Krisch, A. Maljuk, M. Moretti Sala, S. Wurmehl, G. Aslan-Cansever, M. Sturza, L. Hozoi, J. van den Brink, and J. Geck, “Observation of heavy spin-orbit excitons propagating in a nonmagnetic background: The case of $(\text{Ba}, \text{Sr})_2\text{YIrO}_6$,” *Phys. Rev. B* **97**, 064421 (2018).
- [21] Y. Wang, Ruitang Wang, Jung-ho Kim, M. H. Upton, D. Casa, T. Gog, G. Cao, G. Kotliar, M. P. M. Dean, and X. Liu, “Direct Detection of Dimer Orbitals in $\text{Ba}_5\text{AlIr}_2\text{O}_{11}$,” *Phys. Rev. Lett.* **122**, 106401 (2019).
- [22] Hk. Müller-Buschbaum and Ch. Lang, “ $\text{Ba}_5\text{AlIr}_2\text{O}_{11}$: Eine neue Verbindung mit Iridium(IV, V),” *Z. Anorg. Allg. Chem.* **568**, 29–34 (1989).
- [23] J. Terzic, J. C. Wang, Feng Ye, W. H. Song, S. J. Yuan, S. Aswartham, L. E. DeLong, S. V. Streltsov, D. I. Khomskii, and G. Cao, “Coexisting charge and magnetic orders in the dimer-chain iridate $\text{Ba}_5\text{AlIr}_2\text{O}_{11}$,” *Phys. Rev. B* **91**, 235147 (2015).
- [24] See Supplemental Material at [URL].
- [25] M. Moretti Sala, K. Martel, C. Henriquet, A. Al Zein, L. Simonelli, Ch. J. Sahle, H. Gonzalez, M.-C. Lagier, C. Ponchut, S. Huotari, R. Verbeni, M. Krisch, and G. Monaco, “A high-energy-resolution resonant inelastic X-ray scattering spectrometer at ID20 of the European Synchrotron Radiation Facility,” *J. Synchrotron Rad.* **25**, 580–591 (2018).
- [26] Jung-ho Kim, D. Casa, M. H. Upton, T. Gog, Young-June Kim, J. F. Mitchell, M. van Veenendaal, M. Daghofer, J. van den Brink, G. Khaliullin, and B. J. Kim, “Magnetic Excitation Spectra of Sr_2IrO_4 Probed by Resonant Inelastic X-Ray Scattering: Establishing Links to Cuprate Superconductors,” *Phys. Rev. Lett.* **108**, 177003 (2012).
- [27] V. N. Strocov, T. Schmitt, U. Flechsig, T. Schmidt, A. Imhof, Q. Chen, J. Raabe, R. Betemps, D. Zimoch, J. Krempasky, X. Wang, M. Grioni, A. Piazzalunga, and L. Patthey, “High-resolution soft X-ray beamline ADDRESS at the Swiss Light Source for resonant inelastic X-ray scattering and angle-resolved photoelectron spectroscopies,” *J. Synchrotron Rad.* **17**, 631–643 (2010).
- [28] G. Ghiringhelli, A. Piazzalunga, C. Dallera, G. Trezzi, L. Braicovich, T. Schmitt, V. N. Strocov, R. Betemps, L. Patthey, X. Wang, and M. Grioni, “SAXES, a high resolution spectrometer for resonant x-ray emission in the 400 - 1600 eV energy range,” *Rev. Sci. Instrum.* **77**, 113108 (2006).
- [29] X. Lu, P. Olalde-Velasco, Y. Huang, V. Bisogni, J. Pellicciari, S. Fatale, M. Dantz, J. G. Vale, E. C. Hunter, J. Chang, V. N. Strocov, R. S. Perry, M. Grioni, D. F. McMorro, H. M. Rønnow, and T. Schmitt, “Dispersive magnetic and electronic excitations in iridate perovskites probed by oxygen K -edge resonant inelastic x-ray scattering,” *Phys. Rev. B* **97**, 041102 (2018).
- [30] T. Helgaker, P. Jørgensen, and J. Olsen, *Molecular Electronic-Structure Theory* (Wiley, Chichester, 2000).
- [31] Frank Neese, “The ORCA program system,” *WIREs Comput Mol Sci* **2**, 73–78 (2012).
- [32] Celestino Angeli, Renzo Cimiraglia, and Jean-Paul Malrieu, “N-electron valence state perturbation theory: a fast implementation of the strongly contracted variant,” *Chem. Phys. Lett.* **350**, 297 – 305 (2001).
- [33] Jung-ho Kim, M. Daghofer, A. H. Said, T. Gog, J. van den Brink, G. Khaliullin, and B. J. Kim, “Excitonic quasiparticles in a spin-orbit Mott insulator,” *Nature Communications* **5**, 4453 EP – (2014), article.
- [34] H. Gretarsson, J. P. Clancy, X. Liu, J. P. Hill, Emil Bozin, Yogesh Singh, S. Manni, P. Gegenwart, Jung-ho Kim, A. H. Said, D. Casa, T. Gog, M. H. Upton, Heung-Sik Kim, J. Yu, Vamshi M. Katukuri, L. Hozoi, J. van den Brink, and Young-June Kim, “Crystal-Field Splitting and Correlation Effect on the Electronic Structure of A_2IrO_3 ,” *Phys. Rev. Lett.* **110**, 076402 (2013).
- [35] To simulate electron-hole exciton peaks one would need to calculate N-1 (removal of an electron) state calculations.
- [36] Vamshi M. Katukuri, K. Roszeitis, V. Yushankhai, A. Mitrushchenkov, H. Stoll, M. van Veenendaal, P. Fulde, J. van den Brink, and L. Hozoi, “Electronic structure of low-dimensional $4d^5$ oxides: interplay of ligand distortions, overall lattice anisotropy, and spin-orbit interactions,” *Inorg. Chem.* **53**, 4833 (2014).
- [37] See direct product tables for O_h point group representations, e.g. in Ref. [46].
- [38] For example, for pure trigonal distortions, the t_{2g} orbitals

are split into a_{1g} and e_g .

- [39] Sergey V. Streltsov and Daniel I. Khomskii, “Covalent bonds against magnetism in transition metal compounds,” *Proc. Natl. Acad. Sci. USA* **113**, 10491–10496 (2016).
- [40] The canonical orbitals are eigenfunctions of the so-called (effective single particle) Fock operator.
- [41] The orbital compositions are obtained from the Löwdin natural orbital decomposition.
- [42] Per Aake. Malmqvist, Alistair. Rendell, and Bjoern O. Roos, “The restricted active space self-consistent-field method, implemented with a split graph unitary group approach,” *The Journal of Physical Chemistry* **94**, 5477–5482 (1990).
- [43] Sergey V. Streltsov, Gang Cao, and Daniel I. Khomskii, “Suppression of magnetism in $\text{Ba}_5\text{AlIr}_2\text{O}_{11}$: Interplay of Hund’s coupling, molecular orbitals, and spin-orbit interaction,” *Phys. Rev. B* **96**, 014434 (2017).
- [44] Vamshi M. Katukuri and O. V. Yazyev, “Delocalized dimer orbitals in $\text{Ba}_3\text{InIr}_2\text{O}_9$,” to be published.
- [45] Takeshi Sakamoto, Yoshihiro Doi, and Yukio Hinatsu, “Crystal structures and magnetic properties of 6H-perovskite-type oxides $\text{Ba}_3\text{MIR}_2\text{O}_9$ (M=Mg, Ca, Sc, Ti, Zn, Sr, Zr, Cd and In),” *J. Solid State Chem.* **179**, 2595 – 2601 (2006).
- [46] P. W. Atkins, M. S. Child, and C. S. G. Phillips, *Tables for group theory* (Oxford Univ. Press, London, 1993).